REVIEW ARTICLE

CrossMark

Effect of blood glucose level on standardized uptake value (SUV) in ^{18}F- FDG PET-scan: a systematic review and meta-analysis of 20,807 individual SUV measurements

Mahsa Eskian[1,2] · Abass Alavi[3,4] · MirHojjat Khorasanizadeh[1,2] · Benjamin L. Viglianti[5,6] · Hans Jacobsson[7] ·
Tara D. Barwick[8,9] · Alipasha Meysamie[10] · Sun K. Yi[11] · Shingo Iwano[12] · Bohdan Bybel[13] · Federico Caobelli[14] ·
Filippo Lococo[15] · Joaquim Gea[16] · Antonio Sancho-Muñoz[16] · Jukka Schildt[17] · Ebru Tatcı[18] · Constantin Lapa[19] ·
Georgia Keramida[20] · Michael Peters[21] · Raef R. Boktor[22,23] · Joemon John[24] · Alexander G. Pitman[25] ·
Tomasz Mazurek[26] · Nima Rezaei[1,2,27]

Abstract

Objectives To evaluate the effect of pre-scan blood glucose levels (BGL) on standardized uptake value (SUV) in ^{18}F-FDG-PET scan.
Methods A literature review was performed in the MEDLINE, Embase, and Cochrane library databases. Multivariate regression analysis was performed on individual datum to investigate the correlation of BGL with SUV_{max} and SUV_{mean} adjusting for sex, age, body mass index (BMI), diabetes mellitus diagnosis, ^{18}F-FDG injected dose, and time interval. The ANOVA test was done to evaluate differences in SUV_{max} or SUV_{mean} among five different BGL groups (< 110, 110–125, 125–150, 150–200, and > 200 mg/dl).
Results Individual data for a total of 20,807 SUV_{max} and SUV_{mean} measurements from 29 studies with 8380 patients was included in the analysis. Increased BGL is significantly correlated with decreased SUV_{max} and SUV_{mean} in brain ($p < 0.001$, $p < 0.001$,) and muscle ($p < 0.001$, $p < 0.001$) and increased SUV_{max} and SUV_{mean} in liver ($p = 0.001$, $p = 0004$) and blood pool ($p = 0.008$, $p < 0.001$). No significant correlation was found between BGL and SUV_{max} or SUV_{mean} in tumors. In the ANOVA test, all hyperglycemic groups had significantly lower SUVs compared with the euglycemic group in brain and muscle, and significantly higher SUVs in liver and blood pool. However, in tumors only the hyperglycemic group with BGL of > 200 mg/dl had significantly lower SUV_{max}.
Conclusion If BGL is lower than *200 mg/dl* no interventions are needed for lowering BGL, unless *the liver is the organ of interest*. Future studies are needed to evaluate sensitivity and specificity of FDG-PET scan in diagnosis of malignant lesions in hyperglycemia.

Keywords 18F-FDG · PET scan · Blood glucose level · SUV · PET quantification · Diabetes mellitus

Abbreviations

FDG-PET	Fluorodeoxyglucose positron emission tomography
GLUT	Glucose transport protein
FDG-6-P	F-FDG-6- phosphate
glucose-6-P	Glucose-6- phosphate
SNMMI	Society of Nuclear Medicine and Molecular Imaging
EANM	European Association of Nuclear Medicine
mg/dl	Milligram per deciliter
mmol/l	Millimole per liter
SUV	Standardized uptake values
SD	Standard deviation
FBS	Fasting blood sugar
BMI	Body mass index
PET/CT	Positron emission tomography / computed tomography
MD	Mean difference
CI95%	Confidence interval 95%
RBC	Red cell

✉ Abass Alavi
    Abass.Alavi@uphs.upenn.edu

Extended author information available on the last page of the article

Introduction

In recent decades, fluorodeoxyglucose positron emission tomography (FDG-PET) has emerged as a pivotal imaging modality in clinical oncology [1–7]. Currently, thousands of PET scanners have been installed worldwide and are extensively used for diagnosis and staging of malignant tumors [8–12] and assessment of response to radiochemotherapy [13–16]. It is reported that PET results alter staging and treatment management in nearly 40% of patients [17].

The crucial role of FDG-PET scan in cancer imaging is due to its sensitivity in detection of different types of malignant tumors owing to their increased glycolysis and metabolism rate compared with normal tissues [18–21]. Glucose transport proteins (GLUTs) transport glucose and ^{18}F-FDG as its labeled analogue into the cells [22, 23], where they are phosphorylated into glucose-6-phosphate (G-6-P) and ^{18}F-FDG-6-phosphate (FDG-6-P). Unlike G-6-P, ^{18}F-FDG-6-P is not a substrate for G-6-P isomerase; therefore, it is trapped inside the cells and detected by the PET scanner [24–26]. As GLUTs transport both ^{18}F-FDG and unlabeled glucose, it is assumed that in a hyperglycemic state GLUTs will be saturated by excess unlabeled glucose [27–29]; and therefore, secondary to competition between endogenous glucose and ^{18}F-FDG, FDG uptake will reduce in different tissues. Moreover, some of these GLUTs are insulin-dependent transporters such as GLUT4 in skeletal muscle [30, 31], which may facilitate glucose and ^{18}F-FDG cell uptake in patients with high insulin level, and may result in diminishing glucose and ^{18}F-FDG cell uptake in insulin resistance status. Thus, pre-scan hyperglycemia can potentially lead into a distorted tumor-to-target uptake ratio, and hence decrease the sensitivity of the PET scan.

A significant and increasing proportion of patients who undergo PET scan are in a hyperglycemic state. Diabetes [32, 33], medications such as corticosteroids [34, 35] or chemotherapy agents [36, 37], and anxiety [38] are the leading causes of high blood glucose levels (BGL) in patients undergoing PET-scan. In a study of 13,063 patients who underwent FDG-PET scan, pre-scan BGL was higher than 200 mg/dl in 1698 subjects (13%) [32].

Considering the potential effect of pre-scan BGL on FDG uptake, and high prevalence of pre-scan hyperglycemia, different PET scan preparation protocols have tried to define the optimal pre-scan BGL. Society of Nuclear Medicine and Molecular Imaging (SNMMI) [39] guidelines recommend rescheduling the scan if BGL is greater than a wide range of 150–200 mg/dl. European Association of Nuclear Medicine (EANM) [40] guidelines suggest if the plasma glucose level is higher than or equal to 200 mg/dl, the FDG PET/CT study should be rescheduled. EANM guidelines recommend a lower acceptable upper pre-scan BGL for research purposes (i.e., between 126 and 150 mg/dl). Both of these guidelines suggest that pre-scan BGL may be reduced by administration of rapid-acting insulin. However, the EANM guidelines also note the impact of longer-acting insulin, and recommend specific time intervals for acceptable administration of the different acting insulins prior to scan [40]. The inconsistency between different guidelines, which originates from lack of robust and credible evidence, has resulted in a diverse range of accepted pre-scan BGLs in clinical PET imaging. In a Web-based survey of PET/CT users [41], 128 PET users from medical centers in the Americas, Europe, Asia Pacific, and Middle East responded to the question regarding the pre-scan BGL cut-off used in their centers. Cut-off values varied from 150 to 250 mg/dl (8.3–13.9 mmol/l), and 7% of the sites used no cut-off.

The disagreement with regard to the acceptable pre-scan BGL calls for an accurate and evidence-based answer. As mentioned above, considering the potential influence of pre-scan BGL on FDG uptake, hyperglycemia during FDG-PET scan may decrease the sensitivity of FDG-PET in detection of malignant tissue. On the other hand, unnecessary interventions aimed at lowering the BGL are time- and resources-consuming, including insulin injection, which may also increase background FDG uptake and therefore decrease PET scan sensitivity [42]. Moreover, rescheduling the scan is troublesome for patients who need to travel long distances to access PET scan, patients who need urgent examination, and patients who are unwilling to be rescheduled. To the best of our knowledge, no systematic review and meta-analysis has yet quantitatively evaluated the effect of pre-scan BGL on FDG uptake. Herein, through meta-analysis of individual data, we have tried to elucidate the association between pre-scan BGLs and standardized uptake values (SUV), the most frequently used parameter to measure tissue FDG accumulation [43–45].

Methods

This systematic review and meta-analysis study was conducted in accordance with guidelines recommended in Cochrane Handbook for Systematic Reviews [46]. We adhered to the recommendations outlined in the preferred reporting items for systematic reviews and meta-analyses (PRISMA) statement [47] during reporting of the current study's findings.

Literature search

Studies were identified through electronic search of MEDLINE (PubMed), Embase and Cochrane library databases, using a sensitive search strategy. Keywords were selected on the basis of expert opinion, review of literature, and medical subject headings (MeSH), and Excerpta Medica Tree (EMTREE) terms. No limitations were applied for language or year of publications. The initial search was performed in September 2017, and last updated in January 2018. Furthermore, potentially missed additional citations were

manually searched using reference lists of included articles. Identification of unpublished work was attempted by contacting experts and authors of included studies.

We used the following search terms: (positron emission tomography *or* PET *or* positron emission tomography/ computed tomography *or* PET/CT *or* PET-CT *or* suvmax *or* suvmean *or* suvs *or* suv *or* suvaverage *or* "standard uptake value") *AND* (hyperglycaemia *or* hyperglycemia *or* hyperglycemic *or* euglycaemia *or* euglycemia *or* euglycemic *or* "blood glucose" *or* "blood sugar" *or* "plasma glucose" *or* "plasma sugar" *or* "serum glucose" *or* "serum sugar" *or* FBS *or* "glucose level" *or* "sugar level").

Study selection

^{18}F-FDG-PET or ^{18}F-FDG-PET/CT studies that reported SUV (mean or maximum) for any tumor or normal organ were included. Blood glucose level had to be measured prior to PET scan, immediately before the intravenous administration of FDG, after at least 4 h of fasting. All malignant lesions had to be confirmed by biopsy or surgical histopathology. Duplicate reports of the same data, animal studies, case reports, case series with less than ten patients, editorials, and review articles were excluded. Moreover, studies were excluded when there was any condition that could interfere with the relationship between pre-scan BGL and SUVs, including SUVs that were normalized to BGL or lean body mass instead of body weight, or patients who had received insulin or any oral anti-hyperglycemic within 4 h prior to PET scan. Corresponding authors of the included studies were contacted, and asked to provide the raw individual patient data for their study. Mean and standard deviation (SD) of SUV measurements and pre-scan BGL had to be reported individually for each patient. Studies that failed to provide such information were also excluded.

After omitting duplicate citations, two independent reviewers (ME and MHK), blind to the journals and authors, screened titles and abstracts and then full texts to identify studies eligible for inclusion. Disagreements between the reviewers were resolved through joint revision of the article and discussion.

Data collection

Two reviewers independently extracted data from included studies using a pre-specified and piloted data extraction sheet. Disagreements were resolved through discussion between the two authors, and if necessary, a third senior investigator (APM) extracted the data and then discussed the results with reviewers in order to reach consensus.

The following data were extracted from each study: first author's name, year of publication, study design, type of scan (PET or PET/CT), number of patients, number of scans, and duration

of fasting prior to scan. For each individual, the following data were recorded: sex, age, body mass index (BMI), prior diagnosis of diabetes mellitus, type of organ or histology of malignant tumor that underwent PET scan, injected dose of FDG, time interval between FDG administration and imaging, pre-scan BGL, and SUV measurements (SUV$_{max}$ and/or SUV$_{mean}$).

Quality assessment

Two authors independently assessed quality of included studies using Newcastle–Ottawa Scale for cross-sectional and case-control studies [48]. This scale rates studies on three major domains: selection (four scores), comparability (two scores) and ascertainment of outcome of interest (three scores). Studies with between seven and nine scores and between four and six scores were deemed to have low risk and medium risk respectively, and studies gaining three or fewer scores were considered as having a high risk of bias and were excluded from analysis.

Statistical analysis

Regression analysis of individual patient data was performed in order to study the correlation between SUV and pre-scan BGLs. Based on the curve estimation procedure, a linear regression model was the best-fit model for evaluating the relationship between pre-scan BGL and SUV measurements in all organs. Pearson correlation coefficient, as well as β coefficient with confidence interval of 95%, was reported. Multiple linear regression analysis was performed with SUV$_{max}$ or SUV$_{mean}$ as dependent variable and pre-scan BGL, sex, age, BMI, presence of diabetes mellitus diagnosis, injected dose of FDG, and time interval between FDG injection and imaging as independent variables. For ANOVA analysis, patients were categorized into five groups based on pre-scan BGLs: ≤ 109 mg/dl (euglycemia), 110–125 mg/dl (mild hyperglycemia), 126–150 mg/dl, 151–200 mg/dl and > 200 mg/dl. These cut-offs for categorization of BGL were chosen based on suggested pre-scan BGL in SNMMI [39] and EANM [40] guidelines and definition of euglycemia [49]. The ANOVA test was performed to compare SUV$_{max}$ or SUV$_{mean}$ of the four hyperglycemic groups with the euglycemic group, and mean difference along with confidence interval of 95% was reported. All tests were performed for each organ (tumors, muscle, brain, liver, blood pool) separately for SUV$_{max}$ and SUV$_{mean}$. Moreover, SUV$_{max}$ of lung tumors was also analyzed as a separate group in addition to being included in the tumors general group, as it was the only specific type of tumor with sufficient data available for meta-analysis. In all analyses, a *p* value of less than 0.05 was considered statistically significant. STATA version 15.0 software (STATA Corporation, College Station, TX, USA) was used for statistical analysis.

Results

The computerized search of the literature identified a total of 2573 unique citations. After screening the titles and abstracts for eligibility, 330 articles were found to be potentially relevant and were screened at the full text level. A total of 31 studies met all eligibility criteria. Manual search identified one additional unpublished study [50]. Twelve studies already included numerical individual data for 721 SUV measurements. Numerical unpublished individual data from published papers [50–66] were obtained through contacting corresponding authors in 17 studies for 21,122 SUV measurements. Therefore, finally a total of 29 studies provided individual patient data and were included in meta-analysis. Figure 1 is a flow diagram describing the stepwise study selection process according to the PRISMA guidelines.
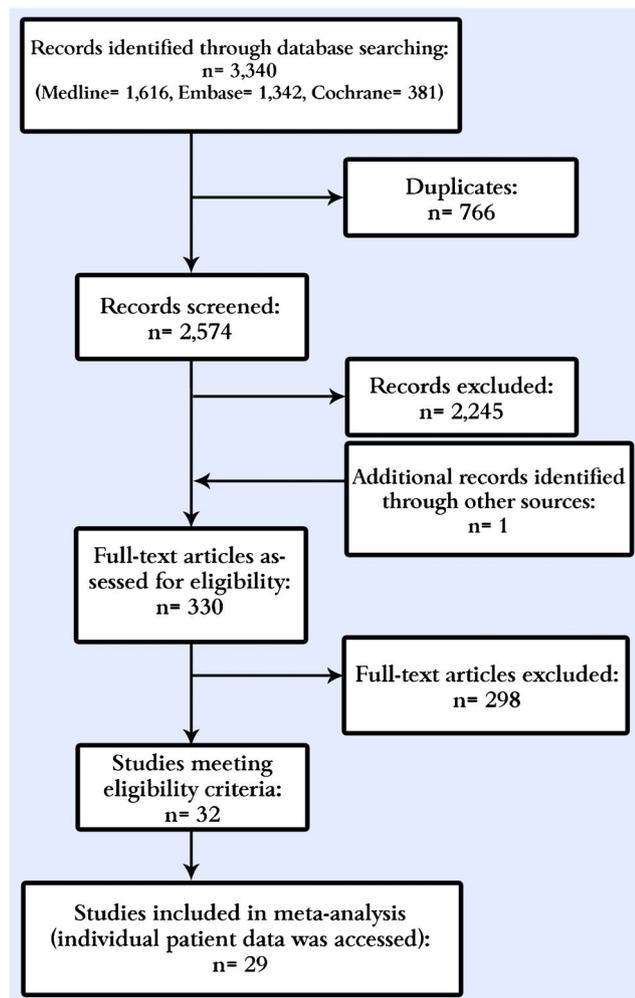

Fig. 1 Flow diagram of the study selection process

Study characteristics and quality assessment

The selected studies included 13 prospective and 16 retrospective studies, reporting a total of 20,807 SUV measurements (total 14,879 SUV_{max} and 5928 SUV_{mean}) in 8380 patients (14.3% hyperglycemic) between 1992 and 2018 (Table 1). Quality assessment of included studies based on the Newcastle–Ottawa Scale indicated that nine out of 29 studies (31%) carried medium risk for bias, and 20 out of 29 studies (69%) were judged to have low risk of bias. Quality assessment did not identify any high-risk study. The main sources of bias were first the use of hospital controls (euglycemic patients) and second, lack of scan reviewer blinding to pre-scan BGL of subjects. Study characteristics as well as results of quality assessment for each included study are summarized in Table 1. Univariate and multivariate regression analysis adjusting for sex, age, BMI, prior diagnosis of diabetes, FDG dose and time interval between FDG injection and imaging were performed in each SUV/organ group. The status of these covariates in each SUV/organ group is described in Table 2.

Clinical outcomes

Tumor

Our data included 631 individual SUV_{max} and 159 individual SUV_{mean} measurements for tumors, including tumors of brain, lung, colorectal, stomach, liver, bone, pancreas, breast, lymphoma, oropharynx, nasopharynx, thyroid, and melanoma. In univariate linear regression analysis (Table 3), pre-scan BGL level had a significant inverse relationship with SUV_{max} ($p < 0.001$, $r = -0.14$, $r^2 = 0.02$) (Fig. 2) and SUV_{mean} ($p = 0.029$, $r = -0.17$, $r^2 = 0.03$). However in multivariate regression analysis (Table 4), no significant relationship was observed between blood glucose and SUV_{max} ($p = 0.948$, $r^2 = 0.61$) and SUV_{mean} ($p = 0.507$, $r^2 = 0.23$). When the regression analyses were restricted to tumors of lung origin (338 individual SUV_{max} measurements), still no significant relationship was found between BGL and SUV in both univariate ($p = 0.079$) and multivariate analysis ($p = 0.505$). ANOVA test for SUV_{max} of tumors revealed that only the group with BGL of more than 200 mg/dl had a significantly lower SUV compared with the euglycemic group (mean difference [MD] =3.49, $p < 0.001$). ANOVA test was not performed for SUV_{mean} of tumor since the number of patients in different BGL groups was not sufficient (Table 5). ANOVA test for SUV_{max} of lung tumors showed no significant differences in SUVs of the euglycemic group compared to different hyperglycemic groups.

Muscle

Our data included 600 individual SUV_{max} and 2156 individual SUV_{mean} measurements for muscle. In univariate

The flow diagram (Fig. 1) contains the following boxes:

- Records identified through database searching: n= 3,340 (Medline= 1,616, Embase= 1,342, Cochrane= 381)
- Duplicates: n= 766
- Records screened: n= 2,574
- Records excluded: n= 2,245
- Additional records identified through other sources: n= 1
- Full-text articles assessed for eligibility: n= 330
- Full-text articles excluded: n= 298
- Studies meeting eligibility criteria: n= 32
- Studies included in meta-analysis (individual patient data was accessed): n= 29

Table 1 Characteristics of included studies

Author/ref	Year	Design	No of patients	Included organs	Risk of bias			
					Selection	Comparability	Outcome	Final score
Sprinz [66]	2018	R	5623	liver, brain	2	2	3	7
Viglianti [63]	2017	R	229	muscle, liver, brain, blood pool	2	1	3	6
Viglianti [50]	2017	R	100	muscle, liver, brain, blood pool	2	1	3	6
Tatcı [61]	2017	R	28	tumor of Hodgkin's lymphoma	2	2	3	7
Cheung [55]	2017	R	19	tumor of oropharynx	2	2	3	7
Werner [53]	2017	R	18	tumor of thyroid	2	2	3	7
Lococo [52]	2016	R	94	tumor of lung	2	1	3	6
Keramida [60]	2015	R	304	liver	2	1	3	6
Rubello [67]	2015	R	50	liver, blood pool	2	1	3	6
Schildt [57]	2015	R	29	liver, blood pool	2	2	3	7
Barwick [65]	2014	R	159	blood pool	2	2	3	7
SanchoMunoz [62]	2014	R	60	muscle	2	1	3	6
Lindholm [56]	2013	R	500	muscle, liver, blood pool	2	1	3	6
Iwano [58]	2013	R	178	tumor of lung	2	2	3	7
Boktor [59]	2013	P	132	liver, blood pool	2	2	3	7
Caobelli [51]	2013	P	130	muscle	2	1	3	6
Garcia [54]	2013	P	120	muscle	2	2	3	7
Mirpour [68]	2012	R	76	tumors of breast, colorectal, head and neck, lymphoma, melanoma, lung	2	2	3	7
Bybel [64]	2011	P	154	liver	2	2	3	7
Harisankar [69]	2011	P	110	liver	2	2	3	7
Huang [70]	2011	P	16	tumor of nasopharynx	2	1	3	6
Janssen [71]	2010	P	30	tumor of rectum	2	2	3	7
Hara [72]	2009	R	54	tumors of liver, bone, lung, pancreas, oral cavity, stomach	2	2	3	7
Nakamoto [73]	2002	P	10	tumor of lung	2	2	3	7
Koyama [74]	2001	P	86	tumor of pancreas	2	2	3	7
Minn [75]	1995	P	10	tumor of lung	2	2	3	7
Minn [76]	1993	P	46	tumor of head and neck	2	2	3	7
Ishizu [77]	1993	P	10	brain and tumor of brain	2	2	3	7
Lindholm [78]	1992	P	5	tumor of head and neck	2	2	3	7

Abbreviations: *No* number, *R* retrospective, *P* prospective

regression analysis (Table 3), an inverse statistically significant relationship was found between BGL and SUV_{max} of muscle ($p < 0.001$, $r = -0.28$, $r^2 = 0.08$). However, this inverse relationship was not statistically significant for SUV_{mean} ($p = 0.124$, $r = -0.03$, $r^2 = 0.001$). In multivariate analysis (Table 4) both SUV_{max} ($p < 0.001$, $r^2 = 0.16$) and SUV_{mean} ($p < 0.001$, $r^2 = 0.63$) were significantly correlated with pre-scan BGL. In ANOVA test for SUV_{max} of muscle, all hyperglycemic groups had significantly lower SUVs than the euglycemic group. However for SUV_{mean} of muscle, this difference was statistically significant for two out of the four hyperglycemic groups (110–125 mg/dl, 125–150 mg/dl, Table 5).

Brain

Our data included 6056 individual SUV_{max} and 457 individual SUV_{mean} measurements for brain. In univariate regression analysis (Table 3) there was a significant inverse correlation between pre-scan BGL and SUV_{max} ($p < 0.001$, $r = -0.42$, $r^2 = 0.18$) (Fig. 3) and SUV_{mean} ($p < 0.001$, $r = -0.58$, $r^2 = 0.34$) (Fig. 4). This significant inverse relationship maintained in the multivariate analysis (Table 4) both for SUV_{max} ($p < 0.001$, $r^2 = 0.31$) and SUV_{mean} ($p < 0.001$, $r^2 = 0.4$). In ANOVA test, SUV_{max} and SUV_{mean} of all hyperglycemic groups were significantly lower than the euglycemic group (Table 5).

Table 2 Descriptive summary of potentially confounding variables included in the multivariate analysis

Organ and SUV type	Total no. of patients	SUV (mean ±SD)	BGL (mean ±SD)	Sex F(M)	Age #	Age Mean ± SD	BMI #	BMI Mean ± SD	Diabetes DM(nDM)	FDG dose (MBq) #	FDG dose (MBq) Mean ± SD	FDG uptake time (min) #	FDG uptake time (min) Mean ± SD
SUV$_{max}$ Tumor	631	7.92 ± 6.26	123.6 ± 52.17	64(172)	321	62.6 ± 11.65	21	24.79 ± 3.09	106(88)	43	364.7 ± 103.37	13	60.08 ± 4.79
SUV$_{mean}$ Tumor	159	7.28 ± 4.79	106.6 ± 39.75	21(59)	79	53.2 ± 14.54	96	24.28 ± 3.81	3(94)	16	334.2 ± 65.16	0	NA
SUV$_{max}$ lung tumor	338	6.94 ± 5.12	112.4 ± 44.9	19(56)	55	65.0 ± 7.75	20	24.79 ± 3.09	28(47)	0	NA	0	NA
SUV$_{max}$ Muscle	600	9.34 ± 5.59	112.12 ± 34.67	9(490)	596	63.8 ± 11.63	484	27.33 ± 5.3	189(410)	500	468.0 ± 48.58	475	64.89 ± 9.27
SUV$_{mean}$ Muscle	2156	2.13 ± 2.58	109.45 ± 31.35	797(1299)	2093	60.1 ± 14.1	488	27.31 ± 5.29	358(1738)	597	434.8 ± 90	2068	62.55 ± 6.79
SUV$_{max}$ Brain	6056	10.77 ± 3.13	112.1 ± 21.5	2801(3254)	5846	57.2 ± 16.67	5985	26.24 ± 4.89	924(5122)	6045	358.5 ± 76.01	428	64.76 ± 9.55
SUV$_{mean}$ Brain	457	6.03 ± 2.15	109.4 ± 36.42	12(444)	453	64.5 ± 10.92	434	27.35 ± 5.45	162(294)	447	468.6 ± 47.6	430	64.74 ± 9.53
SUV$_{max}$ Liver	6680	2.68 ± 0.64	98.2 ± 23.74	2757(3326)	5879	57.4 ± 16.4	6011	26.27 ± 4.82	1025(5312)	6073	361.4 ± 76.39	541	65 ± 9.15
SUV$_{mean}$ Liver	1805	2.39 ± 0.47	109.6 ± 33.21	260(814)	1343	61.4 ± 13.9	829	26.91 ± 5.16	341(1135)	825	418.5 ± 93.61	1062	63.39 ± 7.85
SUV$_{max}$ blood pool	912	2.13 ± 0.5	114.5 ± 32.94	70(812)	879	67.5 ± 10.05	564	27.07 ± 5.12	235(647)	727	441.7 ± 66.66	694	72.28 ± 18
SUV$_{mean}$ Blood pool	1351	1.75 ± 0.44	109.93 ± 30.08	263(816)	1347	61.5 ± 13.84	833	26.95 ± 5.22	264(1062)	829	418.6 ± 93.33	1068	63.32 ± 8.03

Abbreviations: *SUV* standardized uptake values, *BGL* blood glucose level, # number of patients, *BMI* body mass index, *MBq* Megabecquerel, *min* minutes, *SD* standard deviation, *F* female, *M* male, *DM* diabetic, *nDM* non-diabetic, *NA* not available

Table 3 Univariate regression analysis of the correlation between SUV and blood glucose level

SUV and organ	P value	R	R-squared	β coefficient	CI 95%
SUV_{max} tumor	< 0.001	− 0.139	0.019	− 0.017	[− 0.026, − 0.007]
SUV_{mean} tumor	0.029	− 0.173	0.03	− 0.021	[− 0.04, − 0.002]
SUV_{max} lung tumor	0.079	− 0.096	0.009	− 0.011	[− 0.023, 0.001]
SUV_{max} muscle	< 0.001	− 0.283	0.08	− 0.046	[−0.058, −0.033]
SUV_{mean} muscle	0.124	− 0.033	0.001	− 0.003	[− 0.006, 0.001]
SUV_{max} brain	< 0.001	− 0.419	0.176	− 0.061	[− 0.064, − 0.058]
SUV_{mean} brain	< 0.001	− 0.581	0.338	− 0.034	[− 0.039, − 0.03]
SUV_{max} liver	< 0.001	0.251	0.063	0.007	[0.006, 0.007]
SUV_{mean} liver	< 0.001	0.232	0.054	0.003	[0.003, 0.004]
SUV_{max} blood pool	< 0.001	0.2	0.04	0.003	[0.002, 0.004]
SUV_{mean} blood pool	< 0.001	0.282	0.08	0.004	[0.003, 0.005]

Abbreviations: *SUV* standardized uptake values

Liver

Our data included 6680 individual SUV_{max} and 1805 individual SUV_{mean} measurements for liver. In univariate regression analysis (Table 3), a significant and positive correlation was found between pre-scan BGL and both SUV_{max} ($p < 0.001$, $r = 0.25$, $r^2 = 0.06$) and 1805 SUV_{mean} ($p < 0.001$, $r = 0.23$, $r^2 = 0.05$). In multivariate analysis (Table 4), the positive relationship between pre-scan BGL and SUVs remained statistically significant for both SUV_{max} ($p = 0.001$, $r^2 = 0.16$) and SUV_{mean} ($p = 0.004$, $r^2 = 0.2$). In ANOVA test, all four hyperglycemic groups had significantly higher SUV_{max} and SUV_{mean} compared with the euglycemic group (Table 5).

Blood pool

Our data included 912 individual SUV_{max} and 1351 individual SUV_{mean} measurements for blood pool. In univariate regression analysis (Table 3) there was a significant positive correlation between BGL and both SUV_{max} ($p < 0.001$, $r =$
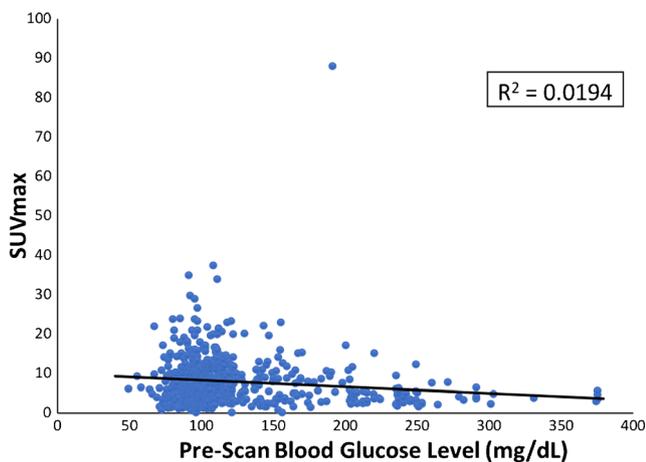
0.20, $r^2 = 0.04$) and SUV_{mean} ($p < 0.001$, $r = 0.28$, $r^2 = 0.08$). This relationship was also statistically significant in the multivariate analysis (Table 4) for both SUV_{max} ($p = 0.008$, $r^2 = 0.29$) and SUV_{mean} ($p < 0.001$, $r^2 = 0.29$). In the ANOVA test, all hyperglycemic groups had significantly higher SUV_{max} and SUV_{mean} in comparison with the euglycemic group, except for the mild hyperglycemic group (110–125 mg/dl) for SUV_{mean} (MD = 0.06, $p = 0.756$) (Table 5).

Discussion

In this meta-analysis of individual data, through multivariate regression analysis, we showed that pre-scan BGL is inversely correlated with SUV in brain and muscle, and positively correlated with SUV in liver and blood pool. However, no significant relationship was found between pre-scan BGLs and SUVs in tumors. When the SUVs of hyperglycemic groups were compared with those of the euglycemic group within each organ, the same pattern was observed, except that when BGL exceeded 200 mg/dl, tumors were associated with significantly lower SUVs compared to the euglycemic group.

Tumor

Based on our multivariate analysis of individual data, pre-scan BGL had a statistically significant effect neither on SUV_{max} and SUV_{mean} of tumors in general, nor on SUV_{max} of lung tumors. The ANOVA test showed that tumors in general had significantly lower SUV_{max} in BGL group of > 200 mg/dl compared with the euglycemic group. However, when the analysis was restricted to only lung tumors, none of the hyperglycemic groups had significantly different SUV_{max} compared with the euglycemic group.

As explained previously, an inverse relationship between pre-scan BGL and tumoral ^{18}F-FDG uptake was expected, due to the presumed competition between FDG and

Fig. 2 Scatter plot of individual SUV_{max} of tumor at different pre-scan blood glucose levels

Table 4 Multivariable regression analysis

SUV and organ	P value BGL	P value DM	P value sex	P value age	P value BMI	P value FDG dose (mbq)	P value FDG uptake time(min)	Overall r	Overall r-squared
SUV_{max} tumor	0.948	0.532	0.928	0.745	0.084	0.133	0.444	0.784	0.614
SUV_{mean} tumor	0.507	0.81	0.728	0.257	0.58	0.388	NA	0.484	0.234
SUV_{max} lung tumor	0.505	0.1	0.971	0.232	0.504	NA	NA	0.628	0.394
SUV_{max} muscle	< 0.001	0.007	0.281	< 0.0001	0.001	0.095	0.002	0.395	0.156
SUV_{mean} muscle	< 0.001	< 0.001	< 0.001	< 0.0001	< 0.0001	<0.0001	< 0.001	0.795	0.633
SUV_{max} brain	< 0.001	0.04	0.245	< 0.0001	< 0.0001	0.335	0.424	0.553	0.306
SUV_{mean} brain	< 0.001	0.081	0.892	0.962	< 0.0001	0.907	0.012	0.636	0.404
SUV_{max} liver	0.001	0.989	0.118	0.055	0.215	<0.001	0.188	0.397	0.157
SUV_{mean} liver	0.004	0.445	0.328	0.017	< 0.0001	0.694	0.105	0.445	0.198
SUV_{max} blood pool	0.008	< 0.001	< 0.001	< 0.001	< 0.001	<0.001	< 0.001	0.759	0.291
SUV_{mean} blood pool	< 0.001	< 0.001	0.385	0.004	< 0.0001	0.507	< 0.001	0.539	0.291

Abbreviations: *SUV* standardized uptake values, *BGL* blood glucose level, *DM* diabetes mellitus, *BMI* body mass index, *MBq* megabecquerel, *min* minutes, *NA* not available

endogenous glucose on the GLUT receptors to enter cells. Although our univariate regression analysis indicated such an effect, in multivariate analysis, after adjusting for several confounding factors, this inverse relationship was not statistically significant. One may speculate that the heterogeneity in nature of included tumors in our study might have differentially affected glucose metabolism rate and FDG uptake. However, even after restricting the analysis to lung tumors, there was still no significant relationship between BGL and SUV_{max} in both univariate and multivariate analysis.

We speculate that these results could be explained by over-expression and augmented capability of glucose transporters in the cellular membranes of tumoral cells [28, 79–82]. In other words, glucose transporters are in such abundance in the malignant tissue that they cannot be saturated even in case of excessive endogenous glucose; thus there is less, if any, competition between FDG and endogenous glucose to enter tumoral cells [83]. Saturation or otherwise is not the issue and would make no difference. Whatever the mechanism of uptake, the proportion of glucose in the circulation that is FDG will decrease the higher the blood glucose; in other words there is always competition, albeit 'passive'. Moreover in normal tissue, glucose metabolism and transportation are controlled by different mechanisms including saturation of GLUTs [22]. However, in malignant tumors transportation and metabolism of glucose lack such controls because of the autonomous nature of malignancies [27, 84]. Thus, hyperglycemia may lead to competition between endogenous glucose and FDG in normal cells but would not have significant effect on tumors.

In the ANOVA test, hyperglycemia with BGL of 110–200 mg/dl was not associated with significantly different SUVs; however the group with BGL of more than 200 mg/dl had significantly lower SUV measurements compared with the euglycemic group. This may be caused by the hexokinase phosphorylation enzymes saturation in the severe hyperglycemia state [85]. Considering the results of the univariate and multivariate regression analyses, this result might be due to the effect of confounding factors. Nevertheless, based on these results we recommend that hyperglycemic patients with BGLs of less than 200 mg/dl are still appropriate candidates to undergo PET scan, as BGL of less than 200 mg/dl would not significantly change tumor's FDG uptake. However, FDG-PET scan of patients with BGL of more than 200 mg/dl should be conducted with more caution.
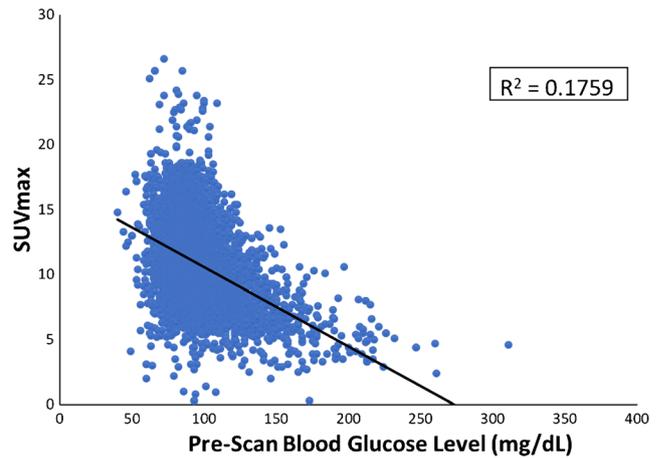
Muscle

In the univariate analysis (Table 3), there was a significant inverse correlation between BGL and SUV_{max} ($p < 0.001$), and no significant correlation between BGL and SUV_{mean} ($p = 0.124$). However, in multivariate regression analysis (Table 4) there was a significant inverse correlation between BGL and both SUV_{max} and SUV_{mean} ($p < 0.001$ for both). In the ANOVA test of SUV_{max}, all of the three hyperglycemic groups had significantly lower SUVs compared with euglycemia. However, for SUV_{mean} two out of the four hyperglycemic groups were significantly different from the euglycemic group (Table 5).

The results of univariate analysis and ANOVA test could be explained by the confounding effect of sex ($p < 0.001$), age ($p < 0.001$), BMI ($p < 0.001$), diabetes ($p < 0.001$), FDG injected dose ($p < 0.0001$), and scan timing ($p < 0.001$). In line with this, studies have indicated that muscle metabolism is age- and sex-dependent [86–88], and the ability of insulin to stimulate glucose transporters in muscles is impaired in diabetes and impaired glucose tolerance [89, 90]. Moreover, patients with higher BMI have more fat tissue, which has a

---

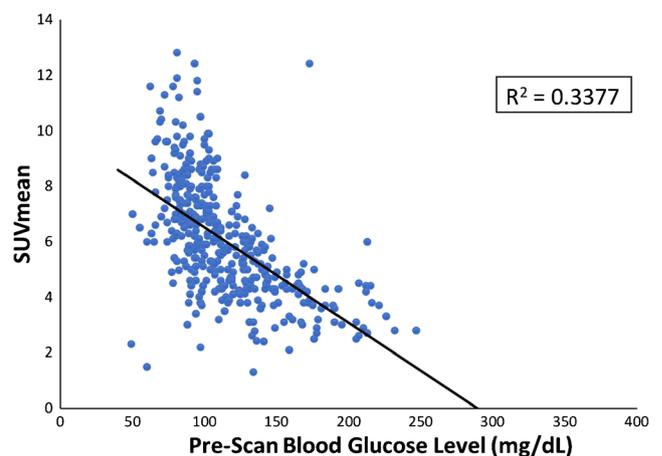**Table 5** ANOVA test comparing SUVs of different blood glucose level groups

SUV and organ	Group 1 ≤109 mg/dl	Group 2 110:125 mg/dl				Group 3 126:150 mg/dl				Group 4 151:200 mg/dl				Group 5: >200 mg/dl			
	#	#	MD	P value	CI 95%	#	MD	P value	CI 95%	#	MD	P value	CI 95%	#	MD	P value	CI 95%
SUV_{max} tumor	367	97	−1.31	0.362	[−3.15, 0.53]	46	0.96	0.913	[−1.32, 3.23]	47	−1.05	1.000	[−6.54, 4.44]	73	3.49	<0.001	[2.32, 4.65]
SUV_{max} lung tumor	242	40	−2.73	0.194	[−6.12, 0.65]	19	0.64	1.000	[−2.74, 4.01]	11	1.94	0.892	[−3.46, 7.33]	25	1.50	0.449	[−0.82, 3.82]
SIV_{max} muscle	356	80	3.16	<0.001	[1.42, 4.89]	90	2.00	<0.001	[0.88, 3.11]	53	3.49	<0.001	[2.27, 4.71]	21	5.01	<0.001	[3.71, 6.32]
SUV_{mean} muscle	1400	328	0.41	0.025	[0.03, 0.78]	225	−0.60	0.006	[−1.09, −0.11]	153	−0.15	0.988	[−0.63, 0.32]	50	0.21	0.967	[−0.37, 0.79]
SUV_{max} brain	4977	585	2.12	<0.001	[1.82, 2.42]	326	3.38	<0.001	[3.04, 3.72]	135	4.93	<0.001	[4.41, 5.45]	33	6.26	<0.001	[5.49, 7.02]
SUV_{mean} brain	255	56	2.00	<0.001	[1.44, 2.55]	82	2.43	<0.001	[1.92, 2.93]	45	3.17	<0.001	[2.43, 3.91]	19	3.56	<0.001	[2.73, 4.39]
SUV_{max} liver	5374	654	−0.17	<0.001	[−0.23, −0.11]	377	−0.43	<0.001	[−0.67, −0.18]	224	−0.51	<0.001	[−0.65, −0.37]	51	−0.64	<0.001	[−0.95, −0.33]
SUV_{mean} liver	1158	247	−0.12	0.004	[−0.22, −0.26]	186	−0.27	<0.001	[−0.37, −0.16]	167	−0.20	<0.001	[−0.31, −0.95]	47	−0.30	<0.001	[−0.48, −0.11]
SUV_{max} blood pool	486	183	0.06	0.756	[−0.54, 0.18]	144	−0.13	0.042	[−0.27, 0.00]	70	−0.27	0.001	[−0.47, −0.08]	29	−0.42	0.008	[−0.75, −0.08]
SUV_{mean} blood pool	859	223	−0.12	0.002	[−0.21, −0.32]	150	−0.31	<0.001	[−0.41, −0.21]	88	−0.29	<0.001	[−0.44, −0.14]	31	−0.47	<0.001	[−0.71, −0.24]

Abbreviations: *SUV* standardized uptake values, *mg/dl* milligram per deciliter, *#* number of SUV records, *MD* mean difference, *CI 95%* confidence interval of 95%

Fig. 3 Scatter plot of individual SUV_{max} of brain at different pre-scan blood glucose levels

relatively low glucose uptake during fasting state [91, 92]. Therefore, a higher proportion of the injected dose of FDG remains in blood and available for uptake by other organs including muscles in obese patients.

Collectively, considering the results of multivariate regression analysis, our study indicates that higher pre-scan BGLs result in lower muscle SUVs (Table 4). This could be explained by the competition between excessive endogenous blood glucose and FDG, and saturation of glucose transporters. However, muscle is known as an insulin-sensitive tissue. The prominent type of muscle glucose transporter is GLUT4, which is insulin-dependent [30, 31, 93], in contrast to tumors which mainly overexpress Glut-1 and Glut-3 transporters, which are not insulin-sensitive [27, 29, 94]. Therefore, one might speculate that hyperglycemic patients would have higher muscle FDG uptake due to insulin secretion and shift of glucose and FDG into muscle cells. This could be a correct assumption in *acute* hyperglycemia (e.g., post-prandial state). However, in our study, all included patients were still hyperglycemic after at least 4 h of fasting

Fig. 4 Scatter plot of individual SUV_{mean} of brain at different pre-scan blood glucose levels

before PET scan. Therefore, they must have had at least some degree of insulin resistance, even though some of them were not yet diagnosed as diabetic patients. As in normal conditions (i.e., no insulin resistance), blood glucose should return to normal levels during the 2 h after ingestion [95, 96]. Several studies have shown that insulin resistance counteracts shifting of glucose to muscle cells by diminishing GLUT4 expression, suppressing glycolysis, and increasing glucose-6-phosphate levels [97–99], all of which lead to increased fasting BGLs. In summary, our results suggest that in patients who are hyperglycemic after at least 4 h of fasting, muscle cells are relatively insensitive to effects of insulin in terms of increasing blood glucose and FDG uptake. Therefore, the competition between excessive endogenous glucose and FDG in entering muscle cells and decreasing GLUT4 expression on cell membrane due to the insulin resistance leads to decreased FDG uptake.

Brain

In both univariate and multivariate analyses, increased pre-scan BGLs resulted in significant decreases in SUV_{max} and SUV_{mean} in brain ($p < 0.001$ for both, Fig. 4). Moreover in the ANOVA test, all hyperglycemic groups had significantly lower SUVs than the euglycemic group for both SUV_{mean} and SUV_{max}. These results also could be explained by the competition of FDG and glucose on the membrane GLUTs in the blood–brain barrier. Moreover the main expressed GLUTs in blood–brain barrier and neurons are GLUT-1 and GLUT-3 which are not insulin-sensitive [100, 101]; thus, hyperinsulinemia during hyperglycemia would not have any effects on FDG uptake in brain.

Liver

In both univariate and multivariate analysis, a positive correlation was found between pre-scan BGLs and both SUV_{max} and SUV_{mean} for liver. Moreover, the ANOVA test showed that this effect of BGL on SUV exists in all hyperglycemic levels since all hyperglycemic groups had significantly higher SUVs compared to the euglycemic group.

Liver is the key organ responsible for regulation of blood glucose through gluconeogenesis and glycogenolysis. During hyperglycemia, liver is the major site of glucose utilization, accounting for uptake of approximately 50% of the ingested glucose [102–104]. In hepatocytes, glucose is phosphorylated by hexokinase to glucose-6-phosphate and then converted to glycogen and stored. Even when the hepatic reserve for glycogen is complete, excess blood glucose is converted into fat by hepatic de novo lipogenesis [105, 106]. Moreover, prominent hepatic GLUT is GLUT-2 which is a bidirectional glucose transporter that allows fluxes of glucose in and out the cells based on its diffusion gradient, and is not a saturable

transporter [107]. Moreover, liver is a highly vascularized organ with high storage of blood [108, 109]. Thus, the effect of hyperglycemia on the ^{18}F-FDG uptake in liver also could be explained by mechanisms affecting the blood pool (see "Blood pool" section below). Therefore as blood glucose increases, liver glucose uptake increases as well since the liver is the main organ responsible for storing excess blood glucose, and this capacity of the liver could overcome the competition between blood glucose and FDG.

Blood pool

In univariate and multivariate analysis of mediastinal blood pool, a direct relationship was found between pre-scan BGL and both SUV_{max} and SUV_{mean} ($p = 0.008$ and $p < 0.001$ respectively). Moreover, in the ANOVA test almost all hyperglycemic groups had significantly higher SUVs than the euglycemic group. It could be explained by the fact that GLUT-1 is the main expressed GLUT in red blood cell (RBC) membrane which is not insulin dependent [22, 110]; thus, insulin resistance would not affect FDG uptake in RBCs. Moreover, it has been shown that chronic hyperglycemia increases the density of GLUTs in RBC membranes [111]. Therefore, RBCs take up more FDG in patients with impaired fasting glucose than in euglycemic patients.

Limitations

Although this systematic review and meta-analysis included 29 studies and 20,807 individual SUVs and pre-scan BGLs, there are some limitations that have to be addressed. First, many of the included studies were of retrospective design, which can potentially lead into selection bias. Although patients in euglycemic and hyperglycemic groups were not paired by sex, age, BMI, injected dose of FDG, time interval between FDG injection and imaging, and diagnosis of diabetes, this information was available for most of the individual data and was taken into account in our multivariate analyses. Nevertheless, there are some other factors theoretically capable of confounding the effect of BGL on SUV that could not be incorporated into our analysis, such as scanner resolution, reconstruction methods, region of interest measurements (a segmentation type processes or a fixed size region for SUV_{mean} of tumors), exact duration of fasting, and serum levels of insulin. Second, we were not able to investigate the effect of BGL on sensitivity and specificity of PET scan in diagnosis of malignant lesions. Third, we were not able to investigate the effect of BGL on tumors separately based on their specific origin and histopathology, except for lung tumors, due to limited data available for each type of tumor.

Clinical points and conclusions

Based on this systematic review and meta-analysis of individual patient data, patients who are still hyperglycemic after at least 4 h of fasting would have significantly lower FDG uptake in brain and muscle and significantly higher FDG uptake in liver and mediastinal blood pool in comparison with euglycemic patients. However, BGL does not have any apparent significant effect on FDG uptake of tumors. Therefore, it seems that FDG uptake ratio of tumor to background normal tissues in which they are located would not decrease during hyperglycemia.

Current available PET-scan preparation protocols suggest rescheduling the scan or consideration of rapid-acting insulin injection prior to PET scan or scan rescheduling in patients with hyperglycemia ranging from 120 mg/dl to 200 mg/dl, and recommend inconsistent and diverse cut-offs for insulin injection or scan rescheduling [39, 40]. This approach may lead to increased costs, inconvenience for patients, unnecessary postponing of PET scan, and delays in diagnosis of potential malignancies, or the possibility of insulin-induced FDG shunting from tumors to muscles, thus decreasing tumor to background FDG uptake ratio [42, 112, 113]. Our results provide credible level 1 evidence on the influence of BGL on FDG uptake, which is much needed in order to reach an evidence-based consensus in regard with preparation protocols needed to handle the issue of hyperglycemia in PET scan.

Considering the lack of significant correlation between BGL and FDG uptake in tumors, we recommend that no interventions — whether insulin injection or scan rescheduling — are needed for hyperglycemic patients who are scheduled to undergo PET scan, except in the following two conditions. First, *BGL > 200 mg/dl*. As our ANOVA analysis indicated decreased FDG uptake of tumors when BGL is above 200 mg/dl, we recommend that BGL be kept under this threshold, as there is the possibility of decreased tumor-to-target uptake ratio and hence impaired scan sensitivity. Second, *when liver is the area of interest.* FDG uptake significantly increases in liver during hyperglycemia for reasons explained above. As our ANOVA tests showed significantly increased SUVs in all ranges of abnormal fasting BGLs — even in the mild hyperglycemic group with blood glucose level of 110–125 mg/dl — we recommend that if feasible, patients should be kept euglycemic (BGL ≤ 110 mg/dl) when assessment of liver is intended , so as to prevent decreased tumor-to-target uptake ratios.

It should be noted that our results and recommendations should not be considered for acute post-prandial hyperglycemia, where influx of FDG into the insulin-sensitive muscle cells results in a so-called "muscle view" in PET scan [42, 114]. Finally, we hope that future controlled prospective studies specifically designed to evaluate sensitivity and specificity of FDG-PET scan in diagnosis of malignant lesions in hyperglycemia compared with euglycemia will further elucidate the effects of BGL on FDG-PET scanning.

Compliance with ethical standards

References

1. Moghbel M, Newberg A, Alavi A. Positron emission tomography: ligand imaging. Handb Clin Neurol. 2016;135:229–40.
2. Basu S, Alavi A. PET-based personalized management in clinical oncology: an unavoidable path for the foreseeable future. PET Clin. 2016;11(3):203–7.
3. Hustinx R, Benard F, Alavi A. Whole-body FDG-PET imaging in the management of patients with cancer. Semin Nucl Med. 2002;32(1):35–46.
4. von Schulthess GK, Steinert HC, Hany TF. Integrated PET/CT: current applications and future directions. Radiology. 2006;238(2):405–22.
5. Rohren EM, Turkington TG, Coleman RE. Clinical applications of PET in oncology. Radiology. 2004;231(2):305–32.
6. Hess S, et al. The pivotal role of FDG-PET/CT in modern medicine. Acad Radiol. 2014;21(2):232–49.
7. Sprinz C, et al. Effects of blood glucose level on 18F-FDG uptake for PET/CT in normal organs: a systematic review. PLoS One. 2018;13(2):e0193140.
8. Volpi S, et al. The role of positron emission tomography in the diagnosis, staging and response assessment of non-small cell lung cancer. Ann Transl Med. 2018;6(5):95.
9. Heiss WD. Positron emission tomography imaging in gliomas: applications in clinical diagnosis, for assessment of prognosis and of treatment effects, and for detection of recurrences. Eur J Neurol. 2017;24(10):1255–e70.
10. Rohde M, et al. 18F-fluoro-deoxy-glucose-positron emission tomography/computed tomography in diagnosis of head and neck squamous cell carcinoma: a systematic review and meta-analysis. Eur J Cancer. 2014;50(13):2271–9.
11. Wu CX, Zhu ZH. Diagnosis and evaluation of gastric cancer by positron emission tomography. World J Gastroenterol. 2014;20(16):4574–85.
12. Fischer BM, Mortensen J. The future in diagnosis and staging of lung cancer: positron emission tomography. Respiration. 2006;73(3):267–76.
13. Bastiaannet E, et al. The value of FDG-PET in the detection, grading and response to therapy of soft tissue and bone sarcomas; a systematic review and meta-analysis. Cancer Treat Rev. 2004;30(1):83–101.

14. Vansteenkiste J, et al. Positron-emission tomography in prognostic and therapeutic assessment of lung cancer: systematic review. Lancet Oncol. 2004;5(9):531–40.

15. Capirci C, et al. Long-term prognostic value of 18F-FDG PET in patients with locally advanced rectal cancer previously treated with neoadjuvant radiochemotherapy. AJR Am J Roentgenol. 2006;187(2):W202–8.

16. Challapalli A, Aboagye EO. Positron emission tomography imaging of tumor cell metabolism and application to therapy response monitoring. Front Oncol. 2016;6:44.

17. Gambhir SS, et al. A tabulated summary of the FDG PET literature. J Nucl Med. 2001;42(5 Suppl):1s–93s.

18. Weber G. Enzymology of cancer cells (first of two parts). N Engl J Med. 1977;296(9):486–92.

19. Hiraki Y, Rosen OM, Birnbaum MJ. Growth factors rapidly induce expression of the glucose transporter gene. J Biol Chem. 1988;263(27):13655–62.

20. Denko NC. Hypoxia, HIF1 and glucose metabolism in the solid tumour. Nat Rev Cancer. 2008;8(9):705–13.

21. Shaw RJ. Glucose metabolism and cancer. Curr Opin Cell Biol. 2006;18(6):598–608.

22. Wood IS, Trayhurn P. Glucose transporters (GLUT and SGLT): expanded families of sugar transport proteins. Br J Nutr. 2003;89(1):3–9.

23. Younes M, et al. Wide expression of the human erythrocyte glucose transporter Glut1 in human cancers. Cancer Res. 1996;56(5):1164–7.

24. Pauwels EK, et al. The mechanism of accumulation of tumour-localising radiopharmaceuticals. Eur J Nucl Med. 1998;25(3):277–305.

25. Khan N, et al. 18F-fluorodeoxyglucose uptake in tumor. Mymensingh Med J. 2011;20(2):332–42.

26. Kumar R, et al. Positron emission tomography imaging in evaluation of cancer patients. Indian J Cancer. 2003;40(3):87–100.

27. Macheda ML, Rogers S, Best JD. Molecular and cellular regulation of glucose transporter (GLUT) proteins in cancer. J Cell Physiol. 2005;202(3):654–62.

28. Brown RS, Wahl RL. Overexpression of Glut-1 glucose transporter in human breast cancer. An immunohistochemical study. Cancer. 1993;72(10):2979–85.

29. Medina RA, Owen GI. Glucose transporters: expression, regulation and cancer. Biol Res. 2002;35(1):9–26.

30. Ishiki M, Klip A. Minireview: recent developments in the regulation of glucose transporter-4 traffic: new signals, locations, and partners. Endocrinology. 2005;146(12):5071–8.

31. Gould GW, Holman GD. The glucose transporter family: structure, function and tissue-specific expression. Biochem J. 1993;295(Pt 2):329–41.

32. Niccoli-Asabella A, et al. 18F-FDGPET/CT: diabetes and hyperglycaemia. Nucl Med Rev Cent East Eur. 2013;16(2):57–61.

33. Cho NH, et al. IDF diabetes atlas: global estimates of diabetes prevalence for 2017 and projections for 2045. Diabetes Res Clin Pract. 2018;138:271–81.

34. Clement S, et al. Management of diabetes and hyperglycemia in hospitals. Diabetes Care. 2004;27(2):553–91.

35. Bonaventura A, Montecucco F. Steroid-induced hyperglycemia: an underdiagnosed problem or clinical inertia? A narrative review. Diabetes Res Clin Pract. 2018;139:203–20.

36. Beyan C, et al. Severe hyperglycemia as a complication of big ICE chemotherapy in a patient with acute myeloblastic leukemia. Haematologia (Budap). 2002;32(4):505–8.

37. Walker ED. Hyperglycemia. A complication of chemotherapy in children. Cancer Nurs. 1988;11(1):18–22.

38. Carrasco-Sanchez FJ, et al. Stress-induced hyperglycemia on complications in non-critically elderly hospitalized patients. Rev Clin Esp. 2018;218(5):223–31.

39. Delbeke D, et al. Procedure guideline for tumor imaging with 18F-FDG PET/CT 1.0. J Nucl Med. 2006;47(5):885–95.

40. Boellaard R, et al. FDG PET/CT: EANM procedure guidelines for tumour imaging: version 2.0. Eur J Nucl Med Mol Imaging. 2015;42(2):328–54.

41. Beyer T, Czernin J, Freudenberg LS. Variations in clinical PET/CT operations: results of an international survey of active PET/CT users. J Nucl Med. 2011;52(2):303–10.

42. Zhao S, et al. Effects of insulin and glucose loading on FDG uptake in experimental malignant tumours and inflammatory lesions. Eur J Nucl Med. 2001;28(6):730–5.

43. Cerfolio RJ, et al. The maximum standardized uptake values on positron emission tomography of a non-small cell lung cancer predict stage, recurrence, and survival. J Thorac Cardiovasc Surg. 2005;130(1):151–9.

44. Weber WA, Schwaiger M, Avril N. Quantitative assessment of tumor metabolism using FDG-PET imaging. Nucl Med Biol. 2000;27(7):683–7.

45. Westerterp M, et al. Quantification of FDG PET studies using standardised uptake values in multi-centre trials: effects of image reconstruction, resolution and ROI definition parameters. Eur J Nucl Med Mol Imaging. 2007;34(3):392–404.

46. Higgins JPT, Green S (editors). Cochrane Handbook for Systematic Reviews of Interventions Version 5.1.0 [updated March 2011]. The Cochrane Collaboration, 2011. Available from: www.handbook.cochrane.org.

47. Liberati A, et al. The PRISMA statement for reporting systematic reviews and meta-analyses of studies that evaluate health care interventions: explanation and elaboration. PLoS Med. 2009;6(7):e1000100.

48. Wells G, Shea B, O'Connell D, Peterson JE, Welch V, Losos M, Tugwell P. The Newcastle-Ottawa Scale (NOS) for assessing the quality of nonrandomised studies in meta-analyses. Ottawa, Ottawa Hospital Research Institute; 2000

49. World Health Organization. Definition and diagnosis of diabetes mellitus and intermediate hyperglycemia. Geneva, World Health Organisation; 2006.

50. Viglianti BL. Plasma glucose effect upon regional brain FDG uptake: implications for semi-quantitative image analysis and dementia classification[abstract]. In: 103rd RSNA Scientific Assembly and Annual Meeting; 2017 November 1, Chicago, SSE16-04. 2017.

51. Caobelli F, et al. Proposal for an optimized protocol for intravenous administration of insulin in diabetic patients undergoing (18)F-FDG PET/CT. Nucl Med Commun. 2013;34(3):271–5.

52. Lococo F, et al. 18F-fluorodeoxyglucose positron emission tomographic scan in solid-type p-stage-I pulmonary adenocarcinomas: what can produce false-negative results? Eur J Cardiothorac Surg. 2017;51(4):667–73.

53. Werner RA, et al. Predictive value of FDG-PET in patients with advanced medullary thyroid carcinoma treated with vandetanib. J Nucl Med. 2017;59(5):756–61.

54. Garcia JR, et al. Influence of subcutaneous administration of rapid-acting insulin in the quality of (18)F-FDG PET/CT studies. Nucl Med Commun. 2014;35(5):459–65.

55. Cheung MK, et al. False positive positron emission tomography / computed tomography scans in treated head and neck cancers. Cureus. 2017;9(4):e1146.

56. Lindholm H, et al. The relation between the blood glucose level and the FDG uptake of tissues at normal PET examinations. EJNMMI Res. 2013;3(1):50.

57. Schildt J, et al. Seasonal temperature changes do not affect cardiac glucose metabolism. Int J Mol Imaging. 2015;2015:916016.

58. Iwano S, et al. What causes false-negative PET findings for solid-type lung cancer? Lung Cancer. 2013;79(2):132–6.

59. Boktor RR, et al. Reference range for intrapatient variability in blood-pool and liver SUV for 18F-FDG PET. J Nucl Med. 2013;54(5):677–82.

60. Keramida G, et al. Quantification of tumour (18) F-FDG uptake: normalise to blood glucose or scale to liver uptake? Eur Radiol. 2015;25(9):2701–8.

61. Tatci E, et al. The correlation between pre-treatment fluorodeoxyglucose positron emission tomography/computed tomography parameters and clinical prognostic factors in pediatric Hodgkin lymphoma. Mol Imaging Radionucl Ther. 2017;26(1):9–16.

62. Sancho-Munoz A, et al. Muscle glucose metabolism in chronic obstructive pulmonary disease patients. Arch Bronconeumol. 2014;50(6):221–7.

63. Viglianti BL, et al. Effect of hyperglycemia on brain and liver (18)F-FDG standardized uptake value (FDG SUV) measured by quantitative positron emission tomography (PET) imaging. Biomed Pharmacother. 2017;88:1038–45.

64. Bybel B, et al. Increased F-18 FDG intestinal uptake in diabetic patients on metformin: a matched case-control analysis. Clin Nucl Med. 2011;36(6):452–6.

65. Barwick TD, et al. 18F-FDG PET-CT uptake is a feature of both normal diameter and aneurysmal aortic wall and is not related to aneurysm size. Eur J Nucl Med Mol Imaging. 2014;41(12):2310–8.

66. Sprinz C, et al. Effects of blood glucose level on 18F fluorodeoxyglucose (18F-FDG) uptake for PET/CT in normal organs: an analysis on 5623 patients. Sci Rep. 2018;8(1):2126.

67. Rubello D, et al. Variability of hepatic 18F-FDG uptake at interim PET in patients with Hodgkin lymphoma. Clin Nucl Med. 2015;40(8):e405–10.

68. Mirpour S, Meteesatien P, Khandani AH. Does hyperglycemia affect the diagnostic value of 18F-FDG PET/CT? Rev Esp Med Nucl Imagen Mol. 2012;31(2):71–7.

69. Harisankar CN, et al. Utility of high fat and low carbohydrate diet in suppressing myocardial FDG uptake. J Nucl Cardiol. 2011;18(5):926–36.

70. Huang B, et al. Dynamic PET-CT studies for characterizing nasopharyngeal carcinoma metabolism: comparison of analytical methods. Nucl Med Commun. 2012;33(2):191–7.

71. Janssen MH, et al. Blood glucose level normalization and accurate timing improves the accuracy of PET-based treatment response predictions in rectal cancer. Radiother Oncol. 2010;95(2):203–8.

72. Hara T, et al. Significance of chronic marked hyperglycemia on FDG-PET: is it really problematic for clinical oncologic imaging? Ann Nucl Med. 2009;23(7):657–69.

73. Nakamoto Y, et al. Reproducibility of common semi-quantitative parameters for evaluating lung cancer glucose metabolism with positron emission tomography using 2-deoxy-2-[18F]fluoro-D-glucose. Mol Imaging Biol. 2002;4(2):171–8.

74. Koyama K, et al. Diagnostic usefulness of FDG PET for pancreatic mass lesions. Ann Nucl Med. 2001;15(3):217–24.

75. Minn H, et al. Lung cancer: reproducibility of quantitative measurements for evaluating 2-[F-18]-fluoro-2-deoxy-D-glucose uptake at PET. Radiology. 1995;196(1):167–73.

76. Minn H, et al. [18F]fluorodeoxyglucose uptake in tumors: kinetic vs. steady-state methods with reference to plasma insulin. J Comput Assist Tomogr. 1993;17(1):115–23.

77. Ishizu K, et al. Effects of hyperglycemia on FDG uptake in human brain and glioma. J Nucl Med. 1994;35(7):1104–9.

78. Lindholm P, et al. Influence of the blood glucose concentration on FDG uptake in cancer–a PET study. J Nucl Med. 1993;34(1):1–6.

79. Guerin C, et al. The glucose transporter and blood-brain barrier of human brain tumors. Ann Neurol. 1990;28(6):758–65.

80. Reske SN, et al. Overexpression of glucose transporter 1 and increased FDG uptake in pancreatic carcinoma. J Nucl Med. 1997;38(9):1344–8.

81. Kato H, et al. Glut-1 glucose transporter expression in esophageal squamous cell carcinoma is associated with tumor aggressiveness. Anticancer Res. 2002;22(5):2635–9.

82. Yang J, et al. GLUT-1 overexpression as an unfavorable prognostic biomarker in patients with colorectal cancer. Oncotarget. 2017;8(7):11788–96.

83. Viglianti BL, et al. Effects of tumor burden on reference tissue standardized uptake for PET imaging: modification of PERCIST criteria. Radiology. 2018;287(3):993–1002.

84. Yamamoto T, et al. Over-expression of facilitative glucose transporter genes in human cancer. Biochem Biophys Res Commun. 1990;170(1):223–30.

85. Arora KK, Pedersen PL. Functional significance of mitochondrial bound hexokinase in tumor cell metabolism. Evidence for preferential phosphorylation of glucose by intramitochondrially generated ATP. J Biol Chem. 1988;263(33):17422–8.

86. Forbes GB, Reina JC. Adult lean body mass declines with age: some longitudinal observations. Metabolism. 1970;19(9):653–63.

87. Gheller BJ, et al. Understanding age-related changes in skeletal muscle metabolism: differences between females and males. Annu Rev Nutr. 2016;36:129–56.

88. Haizlip KM, Harrison BC, Leinwand LA. Sex-based differences in skeletal muscle kinetics and fiber-type composition. Physiology (Bethesda). 2015;30(1):30–9.

89. Bogan JS. Regulation of glucose transporter translocation in health and diabetes. Annu Rev Biochem. 2012;81:507–32.

90. Cline GW, et al. Impaired glucose transport as a cause of decreased insulin-stimulated muscle glycogen synthesis in type 2 diabetes. N Engl J Med. 1999;341(4):240–6.

91. Kershaw EE, Flier JS. Adipose tissue as an endocrine organ. J Clin Endocrinol Metab. 2004;89(6):2548–56.

92. Ferrannini E, et al. Effect of fatty acids on glucose production and utilization in man. J Clin Invest. 1983;72(5):1737–47.

93. Ismail-Beigi F. Metabolic regulation of glucose transport. J Membr Biol. 1993;135(1):1–10.

94. Marom EM, et al. Correlation of FDG-PET imaging with Glut-1 and Glut-3 expression in early-stage non-small cell lung cancer. Lung Cancer. 2001;33(2–3):99–107.

95. Yip WCY, et al. Prevalence of pre-diabetes across ethnicities: a review of impaired fasting glucose (IFG) and impaired glucose tolerance (IGT) for classification of dysglycaemia. Nutrients. 2017;9(11).

96. Simonson GD, Kendall DM. Diagnosis of insulin resistance and associated syndromes: the spectrum from the metabolic syndrome to type 2 diabetes mellitus. Coron Artery Dis. 2005;16(8):465–72.

97. Slieker LJ, et al. Glucose transporter levels in tissues of spontaneously diabetic Zucker fa/fa rat (ZDF/drt) and viable yellow mouse (Avy/a). Diabetes. 1992;41(2):187–93.

98. Kelley DE, et al. The effect of non-insulin-dependent diabetes mellitus and obesity on glucose transport and phosphorylation in skeletal muscle. J Clin Invest. 1996;97(12):2705–13.

99. Kelley DE, Williams KV, Price JC. Insulin regulation of glucose transport and phosphorylation in skeletal muscle assessed by PET. Am J Phys. 1999;277(2 Pt 1):E361–9.

100. Pardridge WM, Boado RJ, Farrell CR. Brain-type glucose transporter (GLUT-1) is selectively localized to the blood–brain barrier. Studies with quantitative western blotting and in situ hybridization. J Biol Chem. 1990;265(29):18035–40.

101. Vannucci SJ, Maher F, Simpson IA. Glucose transporter proteins in brain: delivery of glucose to neurons and glia. Glia. 1997;21(1):2–21.

102. Adeva-Andany MM, et al. Liver glucose metabolism in humans. Biosci Rep. 2016;36(6):e00416.

103. Ferrannini E, et al. The disposal of an oral glucose load in healthy subjects. A quantitative study. Diabetes. 1985;34(6):580–8.

104. Woerle HJ, et al. Pathways for glucose disposal after meal ingestion in humans. Am J Physiol Endocrinol Metab. 2003;284(4): E716–25.

105. Adeva-Andany MM, et al. Glycogen metabolism in humans. BBA Clin. 2016;5:85–100.

106. McDevitt RM, et al. De novo lipogenesis during controlled overfeeding with sucrose or glucose in lean and obese women. Am J Clin Nutr. 2001;74(6):737–46.

107. Karim S, Adams DH, Lalor PF. Hepatic expression and cellular distribution of the glucose transporter family. World J Gastroenterol. 2012;18(46):6771–81.

108. Michels NA. Newer anatomy of the liver and its variant blood supply and collateral circulation. Am J Surg. 1966;112(3):337–47.

109. Selle D, et al. Analysis of vasculature for liver surgical planning. IEEE Trans Med Imaging. 2002;21(11):1344–57.

110. Joost HG, Thorens B. The extended GLUT-family of sugar/polyol transport facilitators: nomenclature, sequence characteristics, and potential function of its novel members (review). Mol Membr Biol. 2001;18(4):247–56.

111. Harik SI, Behmand RA, Arafah BM. Chronic hyperglycemia increases the density of glucose transporters in human erythrocyte membranes. J Clin Endocrinol Metab. 1991;72(4):814–8.

112. Bertoldo A, et al. Interactions between delivery, transport, and phosphorylation of glucose in governing uptake into human skeletal muscle. Diabetes. 2006;55(11):3028–37.

113. James DE. Targeting of the insulin-regulatable glucose transporter (GLUT-4). Biochem Soc Trans. 1994;22(3):668–70.

114. Roy FN, et al. Impact of intravenous insulin on 18F-FDG PET in diabetic cancer patients. J Nucl Med. 2009;50(2):178–83.

Affiliations

Mahsa Eskian[1,2] · Abass Alavi[3,4] · MirHojjat Khorasanizadeh[1,2] · Benjamin L. Viglianti[5,6] · Hans Jacobsson[7] · Tara D. Barwick[8,9] · Alipasha Meysamie[10] · Sun K. Yi[11] · Shingo Iwano[12] · Bohdan Bybel[13] · Federico Caobelli[14] · Filippo Lococo[15] · Joaquim Gea[16] · Antonio Sancho-Muñoz[16] · Jukka Schildt[17] · Ebru Tatcı[18] · Constantin Lapa[19] · Georgia Keramida[20] · Michael Peters[21] · Raef R. Boktor[22,23] · Joemon John[24] · Alexander G. Pitman[25] · Tomasz Mazurek[26] · Nima Rezaei[1,2,27]

1 Research Center for Immunodeficiencies, Children's Medical Center, Tehran University of Medical Sciences, Tehran, Iran

2 Network of Immunity in Infection, Malignancy and Autoimmunity (NIIMA), Universal Scientific Education and Research Network (USERN), Tehran, Iran

3 University of Pennsylvania, Philadelphia, PA, USA

4 Division of Nuclear Medicine, Hospital of the University of Pennsylvania, 3400 Spruce Street, Philadelphia, PA 19104, USA

5 Department of Nuclear Medicine and Molecular Imaging University of Michigan, Ann Arbor, MI, USA

6 Department of Veterans Affairs Healthcare System, Nuclear Medicine Service, Ann Arbor, MI, USA

7 Department of Molecular Medicine and Surgery, Karolinska Institutet, Stockholm, Sweden

8 Department of Imaging, Imperial College Healthcare NHS Trust, London, England

9 Department of Surgery and Cancer, Imperial College, London, England

10 Department of Community and Preventive Medicine, Faculty of Medicine, School of Medicine, Tehran University of Medical Sciences, Tehran, Iran

11 Department of Radiation Oncology, University of Arizona, Tucson, AZ, USA

12 Department of Radiology Nagoya University Graduate School of Medicine, Nagoya, Japan

13 Department of Radiology University of Manitoba, Winnipeg, Canada

14 Department of Nuclear Medicine, Clinic of Radiology and Nuclear Medicine, University Hospital Basel, Basel, Switzerland

15 Department of Thoracic Surgery, Arcispedale Santa Maria Nuova, Reggio Emilia, Italy

16 Hospital del Mar - IMIM. CIBERES, ISCiii, Barcelona, Spain

17 Department of Nuclear Medicine, HUS Medical Imaging Center, Helsinki University Central Hospital, Helsinki, Finland

18 Department of Nuclear Medicine, Chest Diseases and Thoracic Surgery Training and Research Hospital, Ankara, Turkey

19 Department of Nuclear Medicine, University Hospital Würzburg, Würzburg, Germany

20 Department of Nuclear Medicine, Royal Brompton and Harefield Hospital, London, England

21 Brighton and Sussex University Hospitals, NHS Trust, Brighton, England

22 Lake Imaging, St. John of God Hospital, Ballarat, VIC, Australia

23 National Cancer Institute, Cairo University, Giza, Egypt

24 Superintendent Radiographer & RPS PET Centre, Thomas' Hospital, London, England

25 University of Notre Dame, Sydney, NSW, Australia

26 Department of Cardiology, Medical University of Warsaw, Warsaw, Poland

27 Department of Immunology, School of Medicine, Tehran University of Medical Sciences, Tehran, Iran